

EXPERIMENTAL INVESTIGATION OF THE DELAMINATION BEHAVIOR OF GLASS-FIBRE REINFORCED COMPOSITE PIPES

Hocine MAKRI¹, Selma BAALI²

Despite the many benefits that have expanded the field of fiber-reinforced composites applications, they remain vulnerable to failure by fold separation, a failure mode known as delamination. In some applications, fiber-reinforced composites come in the form of tubes for civil use in the underground transport of liquids. Usually these pipes are manufactured using a filament winding technique. Thus, an appropriate selection of the winding angle is therefore required to enhance the delamination resistance. In this paper, the effect of the winding angle and the initial crack length on the delamination behavior of vinyl ester resin-fiberglass composites was investigated experimentally. Accordingly, DCB samples with different winding angles ($\pm 45^\circ$, $\pm 55^\circ$ and $\pm 65^\circ$) were cut from pipes of 08folds manufactured by the filament winding technique and then subjected to tests under mode-I loading. Previously, initial cracks of 50mm and 100mm length were created by the introduction of a thin film of polytetrafluoroethylene (PTFE) during the winding process. The mode-I fracture tests were conducted according to ASTM D5528-94a standards. Results show that the delamination resistance is enhanced with higher winding angles and lower initial crack lengths, respectively. The qualitative analysis shows that $\pm 65^\circ$ winding angle provides the best delamination resistance behavior compared to $\pm 55^\circ$ and $\pm 45^\circ$ winding angles.

Keywords Delamination, Fiber reinforced composite Pipes, Mode- I fracture test, DCB specimens.

1. General

Laminate Glass-Fiber Reinforced Polymer (GFRP) has many competitive advantages compared to metal ones, owing to its good environmental resistance, high specific strength and stiffness, strength-to-weight ratio, low cost, excellent durability, and corrosion resistance [1-3]. All these advantages extend their application field to fluid transportation, where they are used as apparent or underground pipes. Unfortunately, in underground conditions, the GFRP pipes are subjected to delamination under external loads, a mode of frequent damage that

¹ Dr., Department of Mechanical Engineering, Faculty of Technology, University of Msila, Algeria. hocine.makri@univ-msila.dz and LMSM, Laboratory of Materials and Structures Mechanics, University of Msila, Algeria.

² Eng., Department of Mechanical Engineering, Faculty of Technology, University of Msila, Algeria. selma.baali@univ-msila.dz

manifests in a separation of the folds and can lead to ruin in the event of variation[4, 5]. Therefore, studies on delamination in curved structures become of great importance as long as they allow better comprehension of their behavior[6, 7]. However, within a composite structure, several types of delamination can occur depending on the manner in which the displacement of the strands occurs: mode-I, mode-II, and mode-III. For each of them is associated an interlaminar fracture toughness expressed in terms of energy by its corresponding critical energy release rate (G_{Ic} , G_{IIc} , and G_{IIIc}), usually used for quantifying the resistance of the composite material to delamination[8]. Mode-I, denoted by G_{Ic} , refers to a type of loading that leads to the opening of a strand in a material. It is distinguished by its simplicity and the critical energy release rate required for crack propagation, making it associated with the lowest fracture energy. Due to these characteristics, Mode-I is retained as a criterion for delamination tolerance assessment [9, 10]. To characterize the delamination in mode-I loading, the ASTM standards (ASTM D5528 and ISO/DIS 15024) adopt and recommend the use of double cantilever beam specimens (DCB)[11, 12].

It is well known that the behavior of composites reinforced with fibers is affected by several parameters, such as the volume fraction of fibers, the number of folds, and the ply thickness, the sequence of plies, the yarn width, and the winding angle[13–15]. This makes the study of the mechanical behavior of composite tubes reinforced with fibers difficult and important at the same time, to better understand these materials, along with their diverse applications, has driven scientists to explore and innovate, and making it a subject of high research interest. Among them, Davies et al.[16] and Ozdil et al.[17, 18] have experimentally studied the influence of curvature on the delamination of tubes manufactured by filament winding. By comparing G_{Ic} values for samples cut parallel to the tube axis with unidirectional and straight ones, Davies et al. observed no variation in G_{Ic} values for either. Ozdil et al. found a small influence of curvature on G_{Ic} and compliance (C) values when comparing curved (80 mm inner radius) specimens with straight ones, but this influence can be reduced by increasing the laminate thickness. Davies et al. [19] and Leonard et al.[20] investigated the influence of the fiber content on the delamination behavior of laminates. For carbon fiber-reinforced epoxy composites, Davies and Benzeggagh used 61% of gradually increasing fiber volume fractions (12, 24, 36, 48, and 60%). The results of measuring the interlaminar fracture energy in mode I show an important increase in the fracture toughness and critical energy release rate attributed to the fiber bridge formed behind the crack tip. Mahmoudi[9] noticed the effect of fiber bridging on the enhancement of G_{Ic} values.

The effect of the winding angle on the delamination of laminar composites has been considered by several researchers, such as Shetty et al.[21], Mertiny et al.[22], Panuwat Suppakul et al.[15], and Ozdil and Carlsson[18]. All concluded

that multiangle winding significantly affects the strength of tubular composite structures, and a variation in the orientation angle of the fiber with respect to the direction of crack propagation provides high fracture toughness and durability. Furthermore, Ozdil and Carlsson found that multiangle winding produces an increase in G_{Ic} with fiber orientation angle enhancement with respect to the crack propagation direction.

The influence of the stacking sequence and the fiber orientation on the strain energy release rate G_{Ic} was investigated by ArockiaJulias et al.[23], Davallo.[24] and Andra'sSzekre'nyes et al.[11], for a variation from 0° to 90° of the fiber orientation of the four layers near the mid-plane, ArockiaJulias et al. obtained a G_{Ic} enhancement of 50% that they attributed to the fiber bridging and the fiber pull-out. But they attributed the enhanced crack propagation along the fiber surface to the coincidence of the fiber direction with the crack direction. Davallo, attributing the amelioration of the G_{Ic} and G_{IIc} values to the reinforcement mechanisms such as interfacial debonding and fiber bridging. Andra'sSzekre'nyes et al. confirm the contribution of fiber bridging to the resistance to delamination improvement. Moreover, they connect the energy release rate increase with the crack length.

Numerous experimental works related to the delamination of GFRP can be found in the scientific literature; most are addressed to flat and straight DCB specimens [33, 34], but some are addressed to curved GFRP ones, emphasizing the effect of longitudinal curvature on delamination[14, 32]. However, the effect of transverse curvature on delamination is also important and should be examined to better understand delamination behavior according to the loading mode and operating conditions of the tubes[25, 26]. This paper addresses this issue through experimentation. The main objective of this work is to study the delamination of DCB samples with a transverse curvature by focusing on the effect of the winding angle and length of the initial crack on the delamination behavior. Accordingly, specimens cut-out from vinyl ester resin-fiberglass pipes were prepared by filament winding technique and used in this study.

2. Experimental Methods

2.1. Materials

The vinylester/glass specimens used in these experiments were cut from GFRP composite pipes manufactured by the filament winding technique. Based materials used consist of a band of continuous E-glass fiber rovings (E6-type) with 2400Tex of type EDR24-2400-38, supplied by Maghreb Pipe Company (a local company), impregnated with a commercial vinyl ester resin (VE). The use of this thermoset material is due to its very strong bond with glass fibers; it combines very good chemical inertia and high mechanical properties in laminates; and VE is the most commonly used thermoset resin for composite manufacturing purposes such

as storage tanks, pipes, hoods, ducts, and exhaust stacks because of its superior mechanical properties such as corrosion resistance, processability parameters, and toughness higher than polyester resins [27, 12].

The characteristics of roving were provided by the supplier as follows: fiber diameter 22–24 μm , density 2.54 g/cm^3 , tensile strength 2741 MPa, Young's modulus 81.232 GPa, Poisson ratio 0.22, and elongation 4%. The properties of vinylester resin measured at 20°C were: liquid density 1.1 g/cm^3 (ISO 2811), viscosity 374 Cp (Brook FIELD Viscometer with S62 tool at rotational speed of 20 lap/min), and the mechanical properties were determined by tensile testing conducted on five VE specimens prepared following the ASTM D3039 standard guidelines for tensile testing. The specimens were cut to have a consistent rectangular cross-section with dimensions of 250 mm x 25 mm. The tests were performed on a Universal Testing Machine (INSTRON-5969) equipped with a force sensor, accurate to 50 KN, to record the applied load on computer. Tests were performed with a constant crosshead travel speed of 1 mm/min, The mechanical properties determined are presented as follows: limit flexural strength 150 MPa (ISO 178), flexural modulus 3.8 GPa, limit tensile strength 85MPa (ISO R527), and Young's modulus 3.3 GPa (ISO R527).

2.2.Pipes manufacture

The pipes used in the experiment were manufactured by the filament winding technique, as illustrated in Figure 1. It consists of a continuous glass fiber roving, impregnated with a mixture of thermosetting resin and a catalytic system, wound around a rotating mandrel. The GFRP pipe is obtained by the adjustment of two movements, respectively, the rotation of the mandrel and the alternative movement of the glass band guide. After shaping by filament winding, a thermal cure at 150°C for 30 to 40 minutes is necessary while maintaining the rotation of the mandrel. Three winding angles were considered during the manufacture of the tubes ($\pm 45^\circ$, $\pm 55^\circ$ and $\pm 65^\circ$). These winding angles were chosen because they provide the best usage characteristics [22, 14]. Furthermore, a non-adhesive Teflon film made of Polytetrafluoroethylene (PTFE) of 1.3 mm thickness is inserted in the central layer during manufacture (Figure 2). This Teflon film acts as a crack initiator in the midlayer during loading [28]. For this purpose, two initial cracks of 50 mm and 100 mm length were performed by Teflon film insertion during the winding process of composite pipes.

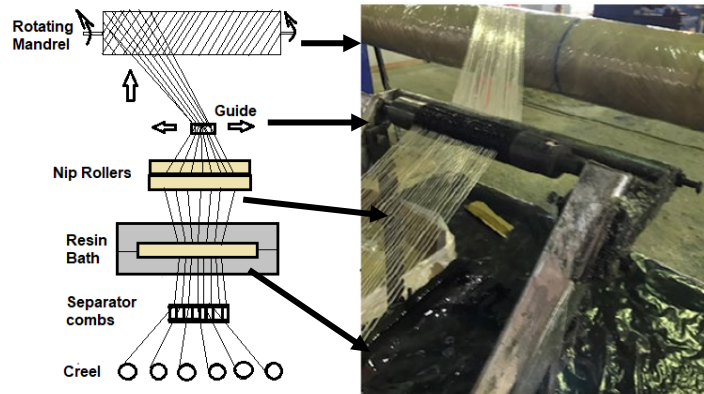


Fig.1. The filament winding process used

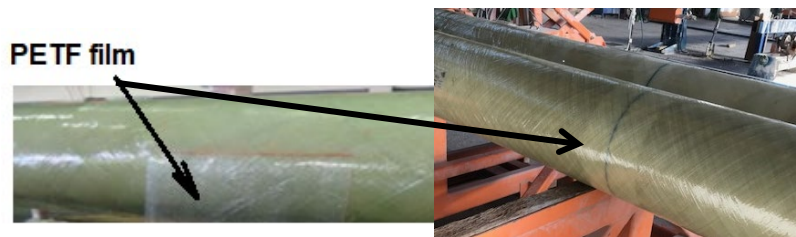


Fig. 2. Crack-initiator film of ‘‘Polytetrafluoroethylene’’ introduced at mid-layer

2.3.Specimens’ preparation

Experimental specimens were cut out of GFR pipes with an inner diameter of 500 mm, as shown in Figure 3. A total of five test specimens were cut for each fiber orientation using a diamond disc saw. The dimensions of the specimens were chosen according to the ASTM D5528-94a standard [29]. Specimens are 200mm in length, 25mm in width, and 5 ± 0.2 mm in thickness, with initial crack lengths of about 55 and 100mm (± 0.2 mm). Furthermore, their surfaces were scrubbed with sandpaper and cleaned carefully. The edges were first flat polished prior to bonding the loading blocks with the araldite adhesive onto the two sides of the specimen. The loading blocks used in delaminating tests were designed according to ASTM D 5528 – 01 (Reapproved 2007)^{e3}.

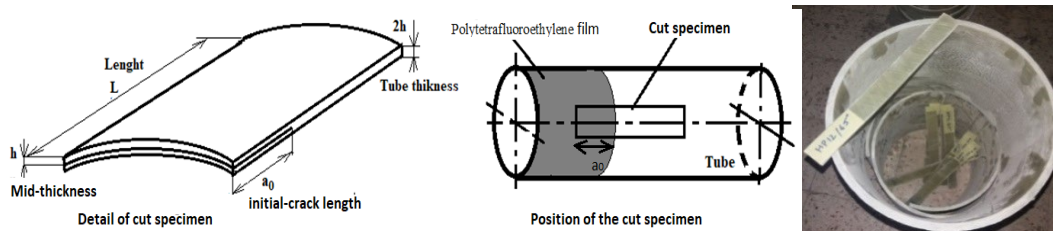


Fig.3. Scheme of cutting operation mode and specimens cut

2.4.Mode-I fracture test

The Mode-I fracture tests were conducted at 20 °C according to ASTM D5528-94a and ISO 15024 standards [29, 30] using a Universal Testing Machine (INSTRON-5969) equipped with a force sensor. The loading capacity of this machine is 50 kN. In order to realize fully crack-opening loads during the tests and avoid moments at the loading point, the load has to be applied in such a manner that the force remains perpendicular to the specimen face. To achieve this objective, a pair of metallic blocks was glued to the end of each specimen (Figure 4). All failure tests were performed at a crosshead speed of 1 mm/min, during which the collected force-displacement ($P-\delta$) values were recorded. An LCD camera connected to a computer is placed in front of the testing machine, allowing the observation and acquisition of instantaneous images and thus facilitating the follow-up of the crack propagation during the test run. The estimation of the size of the initiated cracks that propagate during loading is obtained by drawing an equidistant line of 1mm along the edges of the tested specimen. Furthermore, parts of the specimens recovered after testing were cut out, and their edges were examined using a microscope equipped with a camera and image processing software.

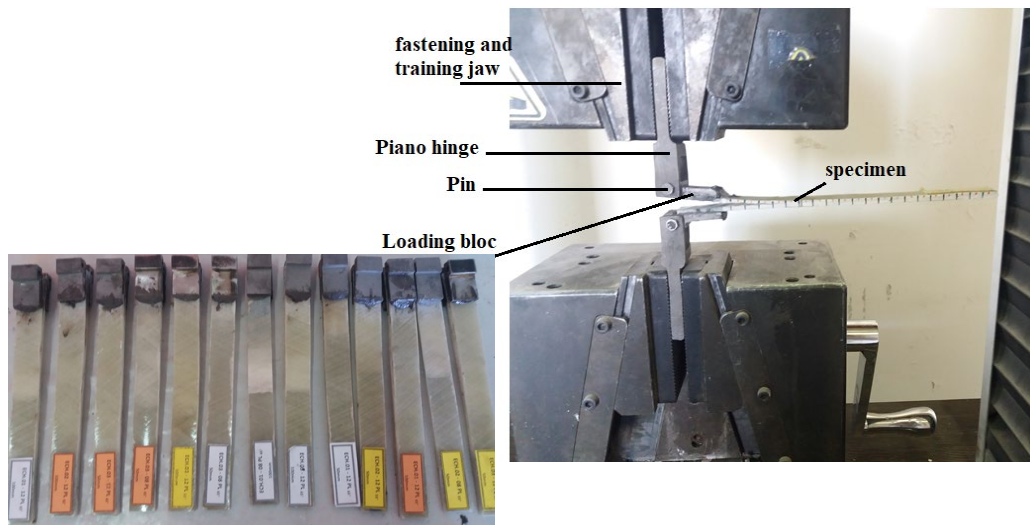


Fig 4.DCB Specimens with blocks glued and experimental device for delamination test

The Compliance Calibration (CC) Method is used to determine the critical energy release rate in Mode-I according to the following formula (Equation. 1):

$$G_{Ic} = \frac{nP\delta}{2ba} \quad (1)$$

Where P , δ , a , and b are the load, the load line deflection, the crack length, and the beam width, respectively. n is an exponent representing the intrinsic parameters of the material.

The compliance, $C = \delta/P$, is calculated through experimental data. It can be expressed as follows:

$$C = m.a^n \quad (2)$$

Where a is the delamination length. m and n are the power law parameters representing the intrinsic parameters of the material. The formula (2) can be rewritten in logarithmic formulation as follows:

$$\text{Log}C = n.\text{Log}a + \text{Log}m \quad (3)$$

Where n is the intrinsic parameters of the material, which can be calculated from the slope of the logC-loga plot.

2.5.R-curve

The R-curve describes the evolution of the delamination resistance or fracture toughness as a function of the crack length. The relation between the effective crack length (a_{eff}) and the interlaminar propagation energy G_{Ip} is determined by the law of compliance as follows:

$$G_{Ip} = \frac{n.P_c^2}{2bk} a_{eff}^{n-1} \quad (4)$$

Where G_{Ip} is the interlaminar propagation energy. a_{eff} is the effective crack length. b the beam width. P_c critical load recorded in propagation phase. n and k are a power law parameter representing material parameters.

3. Results and discussions

The glass volume fraction of samples cut from the pipes used in experiments is determined by the fire loss test technique. It is about 67.52%. This value is considered superior to the nominal value, which was initially set at 55% by the supplier of the pipes. But according to some works [16, 26], the difference in fiber volume fraction between 38 and 70% did not affect it.

3.1. Mechanic tests

Tensile tests were carried out on five specimens at 1.5 mm/min, and the results collected are plotted as load-extension curves presented in figure 5. The results of the tensile test show that the average values of maximum stress for the 45° winding is 36.66 MPa, 43.97 MPa for the 55° winding, and 33.97 MPa for the 65° winding, with diverging strength values. In contrast, the average values of Young modulus relative to the winding angles, which show no disparity in results, are 14.3 GPa for 45°, 13.21 GPa, and 13.57 GPa for 55° and 65°, respectively. This disparity in results suggests that the Young modulus is not affected by the winding angle. However, the 45° winding gives the material more elasticity compared to other inclinations.

The mode-I loading tests were carried out on DCB samples in displacement control. During the course of the tests, the crack growth in all specimens occurred from the crack starter, in the mid-plane of the beams. The force-displacement values ($P-\delta$) collected allowed drawing load-displacement curves. Three representative curves are shown in Figures 6 and 7 respectively to compare their behaviour. The curves are almost identical. Depending on the change in the slope of the curves, three points A, B and C, were marked: they delimit three domains OA, AB and BC on curves.

Domain OA of the graph displays a linear allure, where the load demonstrates a proportional increase relative to the displacement. This aligns with the characteristics of elasticity. However, intermittent minor peaks occasionally disrupt this linear progression, possibly attributed to disparate elastic behaviors between the fibers and matrix during loading. Point A on the graph signifies the conclusion of this linear segment and marks the initiation of cracks.

The subsequent segment of the curve (AB) reveals a rising trend of load concerning displacement, extending until point B. This elevation is thought to be induced by fiber bridging occurring at the crack tip and amidst the strands of the test samples. This bridging phenomenon contributes to an escalation in both load and G_{Ic} values, which is in line with findings from prior research by Davallo [24] and Benzeggagh [19].

In the third phase (BC) of the curves, a diminishing incline punctuated by intermittent peaks indicates a non-linear behavior reminiscent of a "stick-slip" occurrence after the commencement and expansion of delamination. This phenomenon can be attributed to crack jumping between interfaces, which leads to translaminar cracking, as expounded upon in earlier studies [31]. The descent in load accompanying the augmentation of crack growth corresponds to the propagation of delamination, driven by the rupture of the previously mentioned bridged fibers.

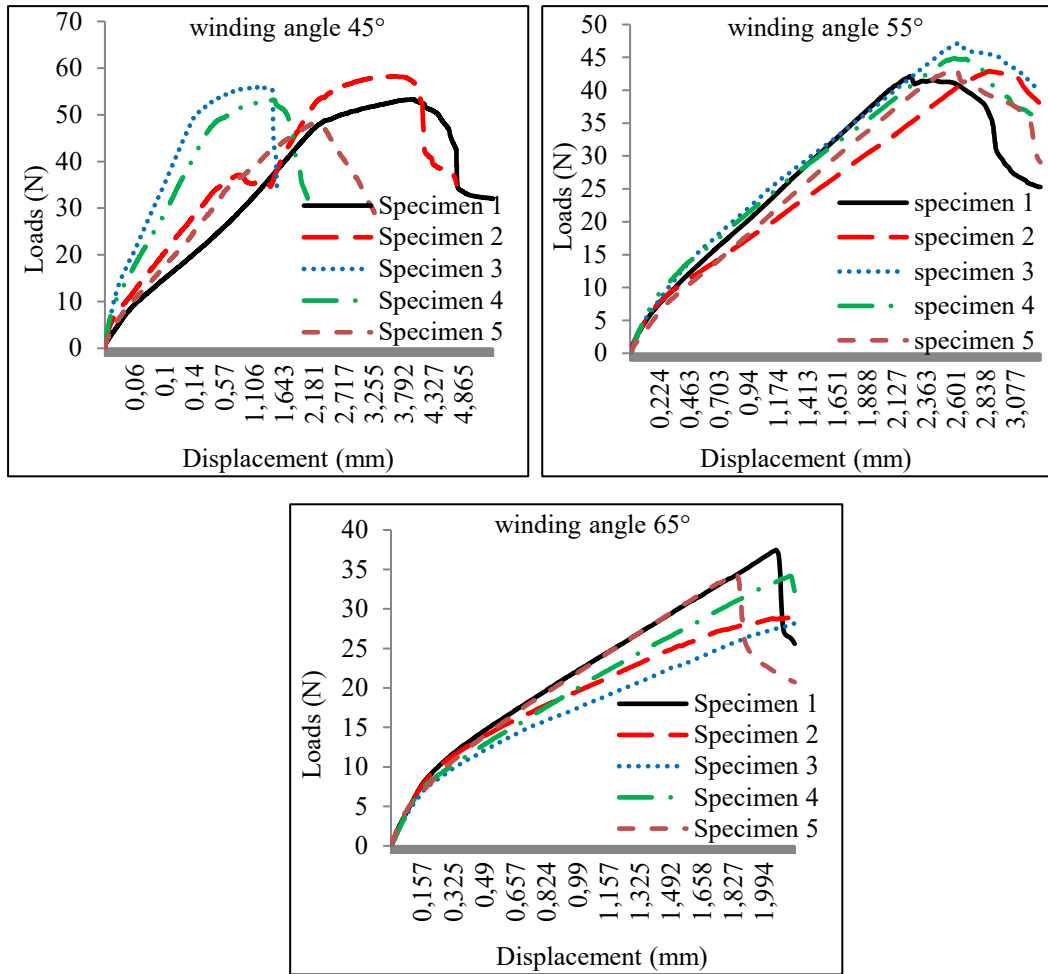


Fig.5. Tensile Load-displacement plots for DCB specimens with different winding angles

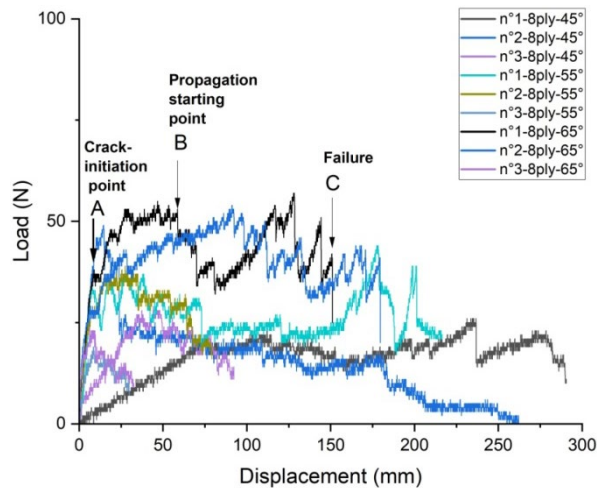


Fig. 6. Load-displacement plots for 50mm of initial crack

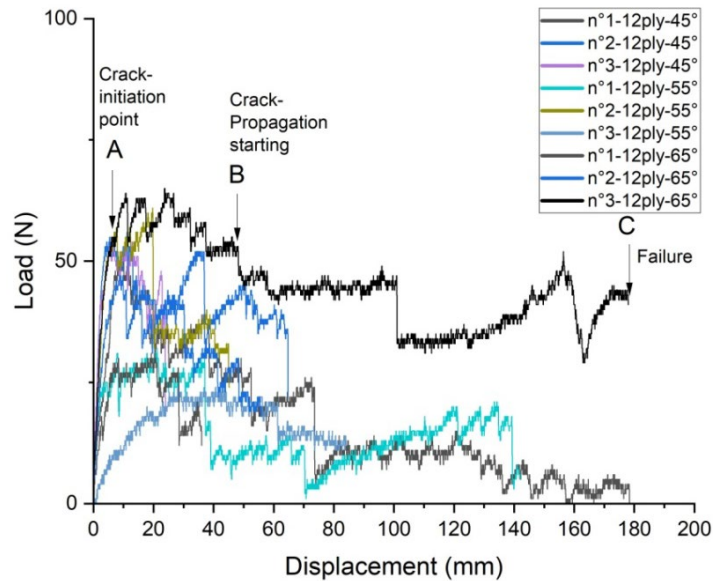


Fig.7. Load-displacement plots for 100mm of initial crack

3.2. Intrinsic parameters of the material

Using the applied load and displacement values for different crack lengths, we can plot the compliance versus delamination growth curves according to formula 3. Figure 8 shows the resulting linear curves. The slope of these curves, denoted as n , can be determined from the corresponding data points. The intrinsic material parameters, n and m , can then be calculated and are presented in Table 1.

Table 1

Values of intrinsic parameters n and m for various fiber winding angles

Winding angle	Intrinsic parameters	
	n	m
$\pm 45^\circ$	1,559	1,97
$\pm 55^\circ$	2,594	3,17
$\pm 65^\circ$	3,641	4,86

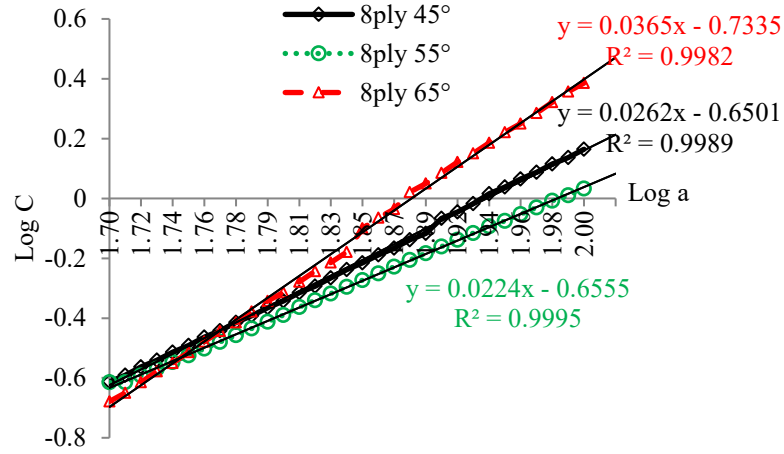


Fig. 8. The compliance versus crack growth curves

3.3.Critical strain energy release rate

Table 2 presents the G_{Ic} values, which are plotted in Figure 9 to show the relationship between winding angles and initial crack length. The G_{Ic} curves show an increasing trend with respect to the increase in winding angle. For specimens with an initial crack length of 50mm, the G_{Ic} values are slightly higher than those of 100mm for winding angles of 45° and 55°. This difference is due to the specimen's lips bending during the test, which causes energy consumption in bending rather than delamination. As the winding angle increases, this bending decreases, resulting in higher G_{Ic} values for the 100mm initial crack curve than the 50mm initial crack curve for a winding angle of 65°. This indicates that a winding angle of ±65° provides better delamination resistance than ±55° and ±45°, respectively. Moreover, an increase in the winding angle relative to the direction of crack propagation enhances the delamination resistance behavior of GFRP pipes.

Table 2

Energy restitution rate G_{Ic} for various winding angles and initial cracks

Winding angle	a_0 (mm)	P_c (N)	δ (mm)	C (mm/N)	G_{Ic} (J/m ²)	G_{Ic} Average (J/m ²)
±45°	50	28,66	21,93	0,76517795	390,379687	300,392033
	100	26,96	25,13	0,93212166	210,404379	
±55°	50	32,01	15,58	0,4867229	515,405891	468,913039
	100	36,89	22,16	0,6007048	422,420188	
±65°	50	34,79	14,68	0,42196033	740,845149	765,685038
	100	15,46	70,5	4,56015524	790,524926	

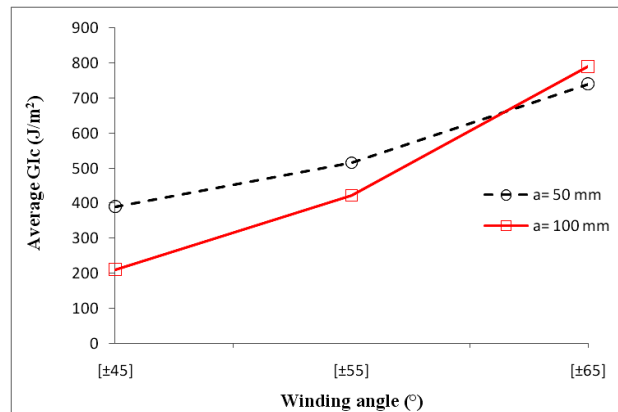


Fig. 9. G_{Ic} with respect the winding angles and initial crack

3.4.R-curve

The R-curve provides insight into the failure process by showing how the cracking energy varies as the crack length evolves. R-curves are plotted based on the winding angles and initial crack length, and are presented in Figure 10. Although the R-curves have similar shapes, there are some discrepancies in their values. The cracking energy shows a monotonic behavior followed by an inflection, and then linear growth with a low slope. The monotonic behavior represents the stability of the fracture behavior during smooth propagation of the crack. The inflection indicates a temporary behavior that results in an increase in cracking energy, which is attributed to the bridging of fibers, a reinforcement that consumes more energy. The linearity in the last part of the curves corresponds to the stability of the crack propagation, but the increasing slope diminishes its importance. A winding angle of 65° provides significantly better delamination resistance behavior than 55° and 45° , which are the most vulnerable angles. The resistance to the initiation of delamination crack depends solely on the initial crack length, indicating that it is an inherent property of the material.

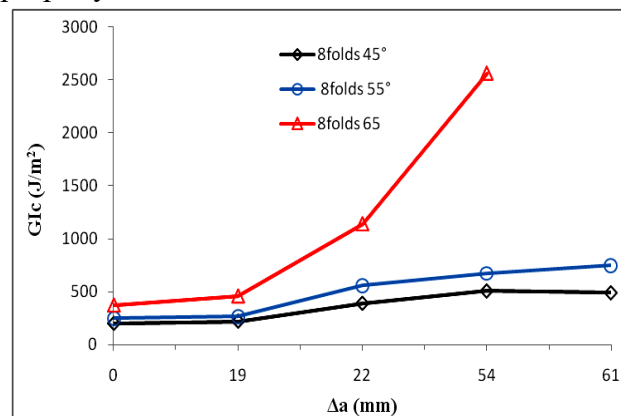


Fig.10. R-curve behaviour

3.5. Microscopic observation

Utilizing a light microscope equipped with an LCD camera and Touptek software, microscopic analyses were conducted. Fractured regions were examined, and micrographs captured in proximity to the crack tips are displayed in Figure 11.

Figures 11.A and B reveals the existence of microcracks within the matrix amidst fibers. These microcracks are likely a consequence of intra-laminar fractures resulting from the bending of distinct plies within the composite during loading. Through a magnification of the fracture vicinity near the crack tip, depicted in Figure 11.C, observable plastic deformation in the matrix encircling the fibers is discernible. This deformation is attributed to the accumulation of an amorphous ductile phase adjacent to the fiber-matrix interface. The presence of this amorphous ductile phase significantly bolsters interfacial bonding by facilitating stress transfer between the matrix and reinforcement.

Figure 11.D portrays the separation of fibers on both sides of the exposed strands, leading to the establishment of fiber bridges connecting these strands. This phenomenon serves as a reinforcement mechanism against delamination and is recognized as a pivotal contributor to the overall structural integrity.

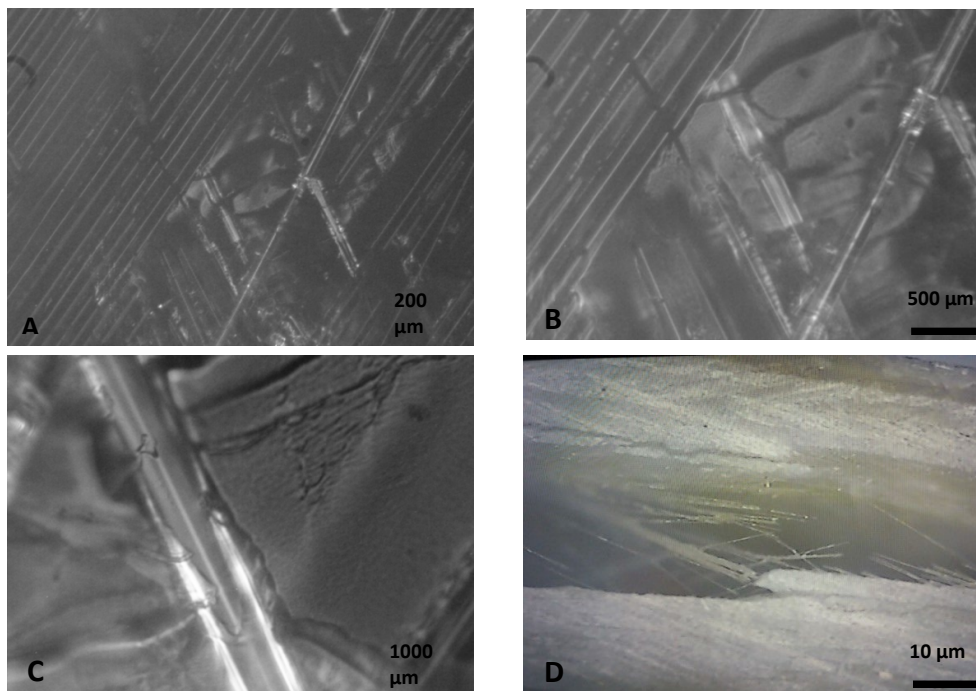


Fig. 11. Micrographs of fractured surfaces (A) and (B); micro cracks formation in the matrix, (C); amorphous phase around the fiber, (D); fibre-bridging between crack flanks

4. Conclusion

The objective of the experimental investigation was to study the behavior of delamination in composite pipes and examine the impact of the fiber orientation angle and initial crack length. The tubes were manufactured using a filament winding process, with varying angles and initial crack lengths. The double-cantilevered beam specimens were transversely oriented and tested under mode I loading conditions. After analyzing and discussing the results, the following conclusions were drawn:

1. A combination of E6 glass fibers and vinyl ester polymer resulted in a composite material with excellent properties, including a Young's modulus of 13.2 to 14.3GPa.
2. The winding angle did not affect the Young's modulus, but it had an impact on the fracture load.
3. The winding procedure used resulted in a high glass content of 67.52%, which exceeded the theoretical values. Although it did not affect the material's mechanical characteristics, optimizing the process is important to reduce the cost of the pipes.
4. Increasing the winding angle in the direction of crack propagation improved delamination resistance, regardless of the number of ply. A winding angle of 65° provided better resistance than 55° and 45° angles, respectively.
5. During the mechanical testing, two phenomena were observed: specimen strands bending and fiber bridging. Specimen strands bending dissipates a significant portion of energy in bending rather than delamination, and its effect increases with the orientation angle. Fiber bridging reinforces against delamination by placing fibers in front of the crack path to delay or slow down its progression. To assess its effect, the number of fibers involved in the bridging and measuring the bridging force needs to be conducted, which was not part of this experiment.
6. The primary degradation mode for the tested pipes was interfacial cracking caused by strands bending during loading. The cracks affected the matrix rather than the fibers, indicating good resistance of the reinforcing fibers against the matrix.

Based on this research, enhancing resistance to delamination in mode I can be achieved by preventing the bending of strands during loading (which is similar to crushing the tubes) and also by minimizing the onset of interfacial rupture. These dual goals can be effectively accomplished by incorporating particles or short fibers into the matrix. This inclusion enhances thickness and creates obstructions or fiber bridging that facilitates lateral reinforcement of the material. Nevertheless, the optimization of the appropriate thickness of composite layers is still necessary to ascertain the ideal short fiber proportions to be adopted.

REFERENCES

- [1]. *TP. Sathishkumar, S. Satheeshkumar and J. Naveen*, Glass fiber-reinforced polymer composites – A review, *Journal of Reinforced Plastics and Composites*, 2014, **33**(13), pp.1258–1275.
- [2]. *Sujith. Bobba, Z. Leman, E.S. Zainuddin and S.M. Sapuan*, Failures Analysis of E- Glass Fibre reinforced pipes in Oil and Gas Industry, A Review, *IOP Conf. Series: Materials Science and Engineering*, 2017, 217:012004.
- [3]. *B. Baali, A. Benmounah, and M. Rokbi*, Mechanical Characterization and Optimum Design of Wound Glass-Fiber-Reinforced Polymer Pipes Based on the Winding Angle and the Number of Plies, *Mechanics of Composite Materials*, 2020, **5**(56): 673-684.
- [4]. *HabibAchache, AbdelouahabBenzerdjeb*, Delamination of a Composite Laminated under Monotonic Loading, *International Journal of Theoretical and Applied Mechanics*, 2017, **2**, pp.119-128.
- [5]. *J.-W. Simon, B. Stier, S. Reese*, Determination of the initiation of delamination in fiber composites, *Blucher Mechanical Engineering Proceedings*, 2014, (1), 1.
- [6]. *W. Beckert, B. Lauke and K. Friedrich*, Delamination Toughness Computation for Curved Thermoplastic Composites, *Applied Composite Materials*, 1995, **1**, pp.395-400.
- [7]. *M. HeidariRarani, M. RafieeAfarani, A. M. Zahedi*, Mechanical characterization of FDM 3D printing of continuous carbon fiber reinforced PLA composites, *Composites Part B: Engineering*, 2019, **175**(15), 107147.
- [8]. *S. Raju and T. K. O'Brien*, "Fracture mechanics concepts, stress fields, strain energy release rates, delamination initiation and growth criteria", in *Delamination Behaviour of Composites*, SrinivasanSridharan, Woodhead Publishing, 2008.
- [9]. *N. Mahmoudi*, Effect of volume fiber and crack length on interlaminar fracture properties of glass fiber reinforced polyester composites (GF/PO composites), *MECHANIKA*, 2014, **20**(2), pp.153-157.
- [10]. *M. M. Shokrieh, M. HeidariRarani, M.R. Ayatollahi*, Delamination R-curve as a material property of unidirectional glass/epoxy composites, *Materials and Design*, 2012, **34**, pp.211–218.
- [11]. *Andra'sSzekre'nyes, Jo'zsef*, Advanced beam model for fiber-bridging in unidirectional composite double-cantilever beam specimens, *Engineering Fracture Mechanics*, 2005, **72**, pp.2686–2702.
- [12]. *ASTM D5528-94a*, Standard Test Method for Mode I Interlaminar Fracture Toughness of Unidirectional Fiber-Reinforced Polymer Matrix Composites, Designation: D5528–01. 2007
- [13]. *X. Jia, G. Chen, Y. Yu, G. Li, J. Zhu, X. Luo, C. Duan, X. Yang, and D. Hui*. Effect of geometric factor, winding angle and pre-crack angle on quasi-static crushing behavior of filament wound CFRP cylinder. *Composites, Part B: Engineering*, 2013, **1**(45), 1336.
- [14]. *RafieeRoham*, Experimental and theoretical investigations on the failure of filament wound GRP pipes. *Composites, Part B: Engineering*, 2013a, **1**(45), pp.257–67.
- [15]. *PanuwatSuppakul, Sri Bandyopadhyay*, The effect of weave pattern on the mode-I interlaminar fracture energy of E-glass/vinyl ester composites, *Composites Science and Technology*, 2002, **62**, pp.709–717.
- [16]. *R. Davies and F. Rannou*, The Effect of Defects in Tubes: Part 1. Mode I delamination Resistance, *Applied Composite Materials*, 1995, **1**, pp.333-349.
- [17]. *F. Ozdil and L.A. Carlsson*, Characterization of Mode I Delamination Growth in Glass/Epoxy Composite Cylinder, *Journal of Composite Materials*, 2000, **34**, 398.
- [18]. *F. Ozdil, and L.A. Carlsson*, Beam analysis of angle-ply laminate DCB specimens, *Composites Science and Technology*, 1999, **59**(2), pp.305-315.

- [19]. *P. Davies and M. L. Benzeggagh*, "Interlaminar Fracture Studies, Chapter 3: Interlaminar Mode-I Fracture Testing", in *Application of Fracture Mechanics to Composite Materials series*, K. Friedrich, Elsevier 1989, **Vol. 6**, pp.81-112.
- [20]. *L.W.H Leonard, K. J. Wong, K.O. Low, and B.F. Yousif*, Fracture behaviour of glass fibre-reinforced polyester composite, *J. Materials: Design and Applications*, 2009, **Vol. 223** Part L, pp.83-89.
- [21]. *M.R. Setty, K.R. Vijay S. Sudir, P. Raghu and D. Madhuranath R.M.V.G. K. Rao*, Effect of fibre orientation on mode I interlaminar fracture toughness of glassy epoxy composites, *Journal of Reinforced Plastics and Composites*, 2000, **19**(08).
- [22]. *P. Mertiny, F. Ellyin, A. Hothan*, An experimental investigation on the effect of multi angle filament winding on the strength of tubular composite structures, *Composites Science and Technology* 2004, **64**(1).
- [23]. *A. ArockiaJulias, R. Rajaraman and Vela Murali*, Effect of fiber orientation on the delamination behaviour of glass-carbon hybrid interface, *International Journal of Mechanical and Production Engineering Research and Development (IJMPERD)*, 2018, **Vol. 8**, Issue 3, pp.1159-1166.
- [24]. *M. Davallo*, Factors Affecting Fracture Behaviour of Composite Materials, *International Journal of Chem Tech Research*, 2010, **2**(4), pp.2125-2130.
- [25]. *G. Wróbel, M. Szymiczek, and J. Kaczmarczyk*, Influence of the structure and number of reinforcement layers on the stress state in the shells of tanks and pressure pipes, *Mechanics of Composite Materials*. 2017, **53**(2).
- [26]. *Rao, D. Srikanth; Reddy, P. Ravinder; Venkatesh, Sriram*, Determination of Mode-I Fracture Toughness of Epoxy-Glass Fibre Composite Laminate, *Procedia Engineering*, 2017, **173**, pp.1678–1683.
- [27]. *G Suresh and LSJayakumari*. Analyzing the mechanical behavior of E-glass fibre-reinforced interpenetrating polymer network composite pipe. *Journal of Composite Materials*, 2000, **0**(0), pp.1–9.
- [28]. *M.S. Sham Prasad, C.S. Venkatesha, T. Jayaraju*, Experimental Methods of Determining Fracture Toughness of Fiber Reinforced Polymer Composites under Various Loading Condition, *Journal of Minerals & Materials Characterization & Engineering*, 2011, **13**(10), 1263.
- [29]. *ISO 15024*, Fibre-reinforced plastic composites determination of mode I interlaminar fracture toughness, G_{Ic} , for unidirectionally reinforced materials, International Organisation for Standardisation, 2001: 24.
- [30]. *P. Compston and P.Y. B. Jar, P. J. Burchill, K. Takahashi*. The Transfer of Matrix Toughness to Composite Mode I Interlaminar Fracture Toughness. in :Glass-Fibre/vinyl Ester Composites.. *Applied Composite Materials*, 2002, 9: 291–314.
- [31]. *M. HeidariRarani, A. Ghadirdokht*. Delamination R-curve behavior of curved compositelaminates. *Composites Part B: Engineering*, 2019, 15(175), pp.107-139.
- [32]. *H.R. Mahdavi, G.H. Rahimi, A. Farrokhhabadi, H. Saadatmand*. Damage Energy Evaluation in [55/-55]₉ Composite Pipes using Acoustic Emission Method. *Mechanics of Advanced Composite Structures*, 2015, 2, pp.127-134.
- [33]. *J. Andersons, M.König*. Dependence of fracture toughness of composite laminates on interface ply orientations and delamination growth direction. *Composites Science and Technology*, 2004, 64, pp.2139–2152.
- [34]. *D. Fanteria, L. Lazzeri, E. Panettieri, U. Mariani, M. Rigamonti*. Experimental characterization of the interlaminar fracture toughness of a woven and a unidirectional carbon/epoxy composite. *Composites Science and Technology*, 2017, 42(1), pp. 20-29.